Thermalization and isotropization of heavy quarks in a non-Markovian medium in high-energy nuclear collisions

Pooja[1], Santosh K. Das,[1] Vincenzo Greco[2,3] and Marco Ruggieri[2,4,*]

[1]*School of Physical Sciences, Indian Institute of Technology Goa, Ponda-403401, Goa, India*
[2]*Department of Physics and Astronomy "Ettore Majorana," University of Catania, Via S. Sofia 64, I-95123 Catania, Italy*
[3]*INFN-Laboratori Nazionali del Sud, Via S. Sofia 62, I-95123 Catania, Italy*
[4]*INFN-Sezione di Catania, Via S. Sofia 64, I-95123 Catania, Italy*

(Received 18 July 2023; accepted 6 September 2023; published 20 September 2023)

We study the isotropization and thermalization of heavy quarks in a non-Markovian medium in high-energy nuclear collisions. In particular, we analyze the case of a nonstationary medium with a noise whose time correlator decays as a power law (heavy-tailed noise). We assume the correlations decay with an exponent $\beta - 1$, $0 \leq \beta < 1$; we treat β as a free parameter. We analyze the effect of memory on the thermalization and isotropization of heavy quarks in the medium via a generalized Langevin equation. In general, we find that memory slows down the dynamics of heavy quarks; moreover, thermalization and isotropization happen on the same timescale once a realistic initialization is considered. We also find that, while the effect on charm quarks can be relevant, beauty quarks are hardly affected by memory in the quark-gluon plasma phase. Finally, we comment on the effect of memory on the estimate of D_s of charm and beauty.

DOI: 10.1103/PhysRevD.108.054026

I. INTRODUCTION

The ultrarelativistic collision experiments performed at the Relativistic Heavy Ion Collider and LHC confirm the existence of a locally equilibrated state of free quarks and gluons known as quark-gluon plasma (QGP) [1–3]. The formation of QGP is a consequence of preequilibrium effects that happen to occur just after the collision of high-energy nuclei. It is assumed that immediately after the collision, the dynamics is that of dense color-electric and color-magnetic fields, namely, the Glasma [4–6] and later, it decays to a system of strongly interacting quarks and gluons, which we call the QGP. The expansion of QGP continues to unbound states of hadrons after which chemical and kinetic freeze-outs take place and the particles fly toward the detectors [7,8].

The dynamics of QGP is governed by light quarks and gluons, along with few heavy quarks. The heavy quarks (HQs) [9–22] are formed very early in the collision experiments and are considered to be effective probes to study the evolution of QGP and Glasma as well. Their large masses m lead to their early production in the medium, $\tau_{\rm prod} \sim 1/m$, hence they can witness the entire evolution of the system from the very beginning of the medium formation. HQs approximately undergo a Brownian motion in a medium of light quarks and gluons [23] and their dynamics can be studied within the framework of Langevin and Fokker-Planck equations, where the interaction is taken care of in terms of diffusion and drag coefficients [23–35].

In the vast majority of the studies related to HQs in QGP, the effects of memory are ignored [17–38]. However, it is plausible to assume that correlations of the forces that act on HQs within the whole evolution of the fireball exist, in particular, when the system approaches the phase transition; moreover, these correlations certainly exist in the early stage, due to the arrangement of the strong gluon fields in the form of correlated domains in the transverse plane [39–41]. Several recent studies [42–52] indicate that the memory effect plays an important role. It was shown in [53] that, even when the memory time is of the order of 1 fm/c, this might have an impact on observables related to HQs, for example, the nuclear modification factor. In [53], a specific form of the noise correlations was assumed, namely, an exponential one, which is characterized by a memory time τ that sets up the scale for the decay of the correlations; there it was also shown that the evolution of HQs is unaffected by memory when their evolution time is much larger than τ.

The purpose of our study is to extend the study of [53] to the case in which the correlations decay with a power law. Such power law correlations appear in different contexts in many areas of physics and chemistry [54–57] and usually

*marco.ruggieri@dfa.unict.it

appear in the presence of strong correlations in the medium: it is therefore worth studying their potential effects on HQs in QGP as well. Different from the case study of [53], we find that HQs can be affected by the presence of correlations even in the late stage of the evolution. In particular, in this study we analyze momentum isotropization and thermalization of HQs in a QGP bath and quantify the effects of memory on these processes. We can anticipate our results here, namely, that not only the presence of memory delays both thermalization and isotropization, but also that the specific form of the noise correlations affect the late time evolution of the system. We estimate the thermalization time of HQs in a bath with memory, both for charm and beauty quarks, finding that charm quarks are more affected than beauty quarks. Finally, from the estimate of the thermalization time, we evaluate the effect of memory on the spatial diffusion coefficient D_s.

The plan of the article is as follows. In Sec. II, we present the formalism and explain how the power law processes are implemented. In Sec. III, we present our results. Finally, in Sec. IV, we summarize our conclusions.

II. FORMALISM

A. Noise with power law memory

In this section, we discuss the method to implement a long-tailed noise whose correlations decay as a power law. We introduce the process

$$h(t) = \sqrt{\kappa}\frac{\sqrt{\beta}}{\tau^{\beta}}\int_0^t (t-u)^{\beta-1}\xi(u)du, \tag{1}$$

where $0 < \beta < 1$; ξ is a standard Gaussian noise with zero average and time correlations given by

$$\langle \xi(t_1)\xi(t_2)\rangle = \tau\delta(t_1 - t_2). \tag{2}$$

We note that Eq. (1) is proportional to the Riemann-Liouville fractional integral of ξ of order β: in fact, besides the overall constant, the process h in (1) corresponds to the formal solution of the fractional Langevin equation $D^{\beta}h = \xi$, where D^{β} denotes the fractional derivative of order β. We introduce the free parameter τ, with dimension of time, so $\tau^{-\beta}$ in front of the integral in Eq. (1) balances the dimension of the integral itself, giving a dimensionless h, and τ balances the dimension of the δ function in Eq. (2) to give a dimensionless ξ. We will show later that τ sets the timescale in the decay of the correlations of h, while β fixes the power law at which correlations decay. The overall $\sqrt{\beta}$ is added for later convenience, to simplify the expressions of the correlator of the noise and of the momentum broadening in the purely diffusive motion. Finally, $\kappa = 1/8.44$ is introduced to reproduce the momentum spreading of the memoryless processes in the limit $\beta \to 0$, see Sec. II C and Fig. 1.

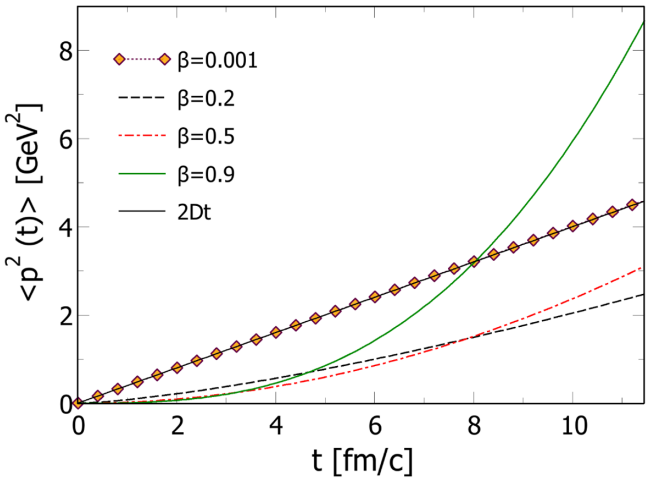

FIG. 1. $\langle p^2\rangle$ versus time for a one-dimensional purely diffusive motion, for several values of β, $\mathcal{D} = 0.2$ GeV^2/fm, and $\tau = 1$ fm/c. We used $1/\kappa = 8.44$ in Eq. (4). For comparison, we show $\langle p^2\rangle = 2\mathcal{D}t$ that would be obtained in the memoryless case. Note that the black solid line and the orange diamonds almost overlap.

The definition (1) has to be understood in the sense of the Itô calculus, namely, it corresponds to

$$h(t_N) = \frac{\sqrt{\beta\kappa}}{\tau^{\beta}}\Delta t\sum_{i=0}^{N-1}(t_N - t_i)^{\beta-1}\xi(t_i), \tag{3}$$

where we assume that the process happens from $t_0 = t_{\text{initialization}}$ to $t_N = t$ in N time steps, each of width $\Delta t = (t_N - t_0)/N$, hence $t_i = t_0 + i\Delta t$. By virtue of Eq. (2) it is easy to prove that the time correlations of h are given by

$$\langle h(t_1)h(t_2)\rangle = \kappa\tau^{-2\beta+1}\beta\int_0^{t_{\min}}(t_1-u)^{\beta-1}(t_2-u)^{\beta-1}du, \tag{4}$$

where $t_{\min} = \min(t_1, t_2)$. The integral on the right-hand side of Eq. (4) can be expressed in terms of an incomplete Euler beta function, namely,

$$\langle h(t_1)h(t_2)\rangle = \kappa\tau^{-2\beta+1}\beta(t_1 - t_2)^{2\beta-1}(-1)^{-\beta}B_Z(\beta,\beta), \tag{5}$$

with $Z = -t_2/(t_1 - t_2)$ and

$$B_Z(x,y) = \int_0^Z u^{x-1}(1-u)^{y-1}du. \tag{6}$$

It is easy to see that for $t_1 \gg t_2$ the correlator (4) decays as a power law. In fact, in the limit $t_1 \gg t_2$ the factor $(t_1 - u)$ in the integral in Eq. (4) can be replaced by t_1, so that

$$\langle h(t_1)h(t_2)\rangle \approx \kappa\tau^{-2\beta+1}\beta t_1^{\beta-1}\int_0^{t_2}(t_2-u)^{\beta-1}du = \kappa\left(\frac{t_1}{\tau}\right)^{\beta-1}\left(\frac{t_2}{\tau}\right)^{\beta}. \quad (7)$$

We note that $\beta > 0$ is enough to ensure the convergence of the integral above. Thus, for fixed t_2, the correlations of the process (1) decay for $t_1 \gg t_2$ with the power law $1/t_1^{1-\beta} \approx 1/(t_1-t_2)^{1-\beta}$: the smaller β implies the faster decay of correlations. Since time correlations in h exist, we say that this process has a memory; moreover, since the time correlations decay with a power law, we say that the process is characterized by a long-tailed memory, to distinguish it from the processes studied before in which the correlations are damped exponentially. Sometimes these processes are called heavy-tailed processes, to emphasize that the correlations of the noise do not decay exponentially with time. We also note that the correlator does not depend on $t_1 - t_2$ but on t_1 and t_2 separately. This will lead to a nonstationary Langevin equation in the next section.

The δ function in Eq. (2) has to be understood as $\delta_{t_1,t_2}/\Delta t$. Consequently, it is convenient to rescale ξ as

$$\xi(t) = \sqrt{\frac{\tau}{\Delta t}}\zeta(t), \quad (8)$$

so that ζ is generated at each time step according to

$$\langle \zeta(t_1)\zeta(t_2)\rangle = \delta_{t_1,t_2}. \quad (9)$$

By virtue of the rescaling (8), we can rewrite Eq. (3) as

$$h(t_N) = \tau^{-\beta+1/2}\sqrt{\kappa\beta\Delta t}\sum_{i=0}^{N-1}(t_N - t_i)^{\beta-1}\zeta(t_i), \quad (10)$$

where $\zeta(t)$ corresponds to white noise with variance equal to 1.

B. Generalized Langevin equation

In our study, we couple the noise h discussed in the previous subsection to heavy quarks via a generalized Langevin equation: for simplicity, we present the formulation of a one-dimensional motion, while actual numerical calculations will be run for the three-dimensional case.

The Langevin equation for momentum p reads [58–68]

$$\frac{dp(t)}{dt} = -\int_0^t dt'\gamma(t,t')p(t') + \eta(t), \quad (11)$$

where the integral term represents the dissipative force and $\eta(t)$ is the thermal noise in a bath at the temperature T. We note that we assume the dissipative kernel γ is a function of both t and t': this is called an irreversible generalized Langevin equation [58–69], as it generalizes the Langevin equation to the motion of probes in nonstationary baths that are characterized, for example, by time and/or space changes in the bath temperature. In heavy ion collisions, modeling a $\gamma = \gamma(t,t')$ could be relevant, because the medium evolution is not invariant under time translations even though the system is locally in thermal equilibrium.

Following the notation of [53] we assume that $\eta(t)$ in (11) satisfies

$$\langle \eta(t)\rangle = 0, \quad (12)$$

$$\langle \eta(t_1)\eta(t_2)\rangle = 2\mathcal{D}\frac{g(t_1,t_2)}{2\tau}, \quad (13)$$

where $\mathcal{D}$ is the diffusion coefficient and g is a dimensionless function that defines the correlation of the noise; the factor $1/2\tau$ in Eq. (13) is introduced to balance the dimension of $\mathcal{D}$ so that the dimensions of the left- and the right-hand sides of the equation match. In the case of a Markov process, $g(t)/2\tau = \delta(t)$. We put

$$\eta(t) = \sqrt{\frac{\mathcal{D}}{\tau}}h(t), \quad (14)$$

where h is the process introduced in Sec. II A. Hence,

$$\langle \eta(t_1)\eta(t_2)\rangle = \frac{\mathcal{D}}{\tau}\langle h(t_1)h(t_2)\rangle, \quad (15)$$

where the correlator on the right-hand side is given by Eq. (4). The comparison with Eq. (13) gives

$$g(t_1,t_2) = \langle h(t_1)h(t_2)\rangle. \quad (16)$$

In terms of h, the Langevin equation (11) becomes

$$\frac{dp(t)}{dt} = -\int_0^t dt'\gamma(t,t')p(t') + \sqrt{\frac{\mathcal{D}}{\tau}}h(t). \quad (17)$$

The time-discretized version of this equation reads

$$\Delta p = -\Delta t\int_0^t dt'\gamma(t,t')p(t') + \sqrt{\frac{\mathcal{D}}{\tau}}h(t)\Delta t. \quad (18)$$

The dissipative term in Eq. (18) has to be understood as an Itô integral; we can then rewrite Eq. (18) as

$$p(t_N) = p(t_{N-1}) - \Delta t\sum_{k=0}^{N-1}\gamma(t_N,t_k)p(t_k)\Delta t + \sqrt{\frac{\mathcal{D}}{\tau}}h(t_N)\Delta t, \quad (19)$$

with $t_0 = t_{\text{initialization}}$, $t_N = t$, and $t_{N-1} = t_N - \Delta t$.

We define the kernel of the dissipative force as

$$\gamma(t,t') = \frac{\mathcal{D}}{E(t_k)T}\frac{\langle h(t)h(t')\rangle}{\tau}, \tag{20}$$

where we took into account the rescaling (14); we put $E = \sqrt{\boldsymbol{p}^2 + m^2}$ and m is the heavy quark mass. The definition (20) is inspired by the Einstein relation between the drag and the diffusion coefficient in a medium [23,64,70,71]. Equations (10), (19), and (20) represent the whole process we implement in our study.

When we compare the results of the process $p(t)$ in Eq. (11) with a memoryless process, we replace

$$\frac{g(t_1,t_2)}{2\tau} \to \delta(t_1 - t_2) \tag{21}$$

in Eq. (13); hence correlations of the noise in this case read

$$\langle \eta(t_1)\eta(t_2)\rangle = 2\mathcal{D}\delta(t_1 - t_2) = \frac{2\mathcal{D}}{\Delta t}\delta_{t_1,t_2}. \tag{22}$$

Instead of Eq. (20), we then have

$$\gamma(t,t') = \frac{2\mathcal{D}}{ET}\delta(t - t') \equiv 2\gamma\delta(t - t'); \tag{23}$$

the overall 2 on the right-hand side of the above equation takes into account that the integration over t' in (17) is over the range $(0,t)$, so the δ function has its support at the upper integration limit, and

$$\int_0^t dt'\delta(t - t') = \frac{1}{2}. \tag{24}$$

Hence, Eq. (11) becomes

$$\frac{dp(t)}{dt} = -\gamma p(t) + \eta(t). \tag{25}$$

Adopting the standard rescaling of the noise

$$\eta(t) = \sqrt{\frac{2\mathcal{D}}{\Delta t}}\xi, \tag{26}$$

we can rewrite Eq. (25) as

$$\Delta p = -\gamma p\Delta t + \sqrt{2\mathcal{D}\Delta t}\xi, \tag{27}$$

where ξ is a Gaussian noise with $\langle\xi\rangle = 0$ and $\langle\xi^2\rangle = 1$.

C. Purely diffusive motion and determination of κ

It is useful to compute the evolution of $\langle p^2(t)\rangle$ in a purely diffusive, one-dimensional motion,

$$\frac{dp(t)}{dt} = \eta(t), \tag{28}$$

with $\langle\eta(t)\rangle = 0$ and

$$\langle \eta(t_1)\eta(t_2)\rangle = \frac{\mathcal{D}}{\tau}\langle h(t_1)h(t_2)\rangle, \tag{29}$$

in agreement with the discussion in the previous subsection. For the purpose of the present section, it is enough to assume that the initial momentum is $p_0 = 0$: if $p_0 \neq 0$ then $\langle p^2(t)\rangle$ should be replaced by $\langle (p(t) - p_0)^2\rangle$. From (28) we have

$$\langle p^2(t)\rangle = \frac{\mathcal{D}}{\tau}\int_0^t dt_1 \int_0^t dt_2 \langle h(t_1)h(t_2)\rangle. \tag{30}$$

In the above integral, the correlator to be used is given by Eq. (4).

In Fig. 1 we plot $\langle p^2\rangle$ versus time for several values of β, $\mathcal{D} = 0.2$ GeV^2/fm, and $\tau = 1$ fm/c. The value of $\mathcal{D}$ has been chosen in agreement with the perturbative quantum chromodynamics (pQCD) value at $T = 1$ GeV. We note that initially, for higher β, slower diffusion occurs. On the other hand, for $t \gg \tau$ the trend is inverted and larger β implies a faster diffusion. In particular, for the smallest value of β shown in the figure, $\langle p^2(t)\rangle$ evolves almost linearly with time, in agreement with our previous discussion, while for larger β the $\langle p^2(t)\rangle$ increases with a power of time larger than 1. We also note that for $\beta \to 0$ the momentum broadening agrees with the one that would be obtained in a bath without memory, namely, $\langle p^2\rangle = 2\mathcal{D}t$: as we show later, this result is independent of τ.

We were able to extract an approximate analytical expression for the time dependence of $\langle p^2(t)\rangle$: using Eq. (7) on the right-hand side of Eq. (30), we get

$$\begin{aligned}\langle p^2(t)\rangle = {} & \frac{\kappa\mathcal{D}}{\tau}\tau^{-2\beta+1}\int_0^t dt_1 \int_0^{t_1} dt_2 t_1^{\beta-1}t_2^{\beta} \\ & + \frac{\kappa\mathcal{D}}{\tau}\tau^{-2\beta+1}\int_0^t dt_1 \int_{t_1}^t dt_2 t_2^{\beta-1}t_1^{\beta},\end{aligned} \tag{31}$$

where we used the fact that the form (7) stands for $t_1 > t_2$, so a similar result needs to be used for the case $t_2 > t_1$ in (30). Performing the elementary integration, we then have

$$\langle p^2(t)\rangle = \frac{2\kappa\mathcal{D}}{1 + 3\beta + 2\beta^2}\left(\frac{t}{\tau}\right)^{2\beta} t. \tag{32}$$

In Fig. 2 we compare the result (32) with the full calculation (30) on a log-log scale. We note that the approximation (32) does not work well for small values of β, while it works pretty well for $\beta \approx 1$. However, it is remarkable that the slopes of the approximate and exact solutions agree with each other in the whole range of β. Hence, while Eq. (32)

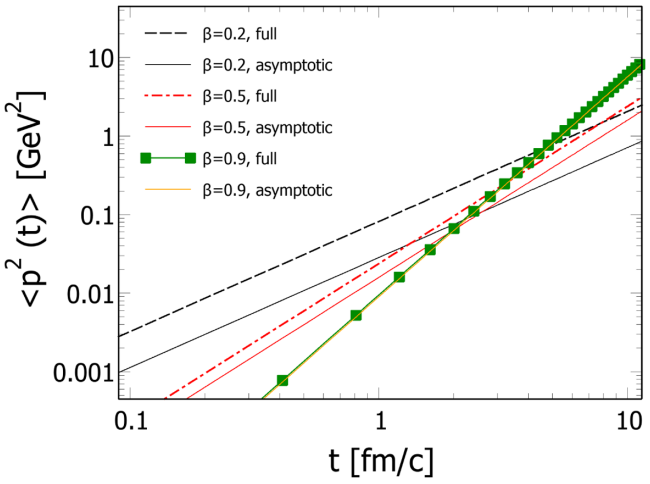

FIG. 2. $\langle p^2 \rangle$ versus time for a one-dimensional purely diffusive motion, for three different values of β, $\mathcal{D} = 0.2$ GeV^2/fm, and $\tau = 1$ fm/c. The asymptotic form corresponds to Eq. (32). Note that the green squares and the thin orange line overlap.

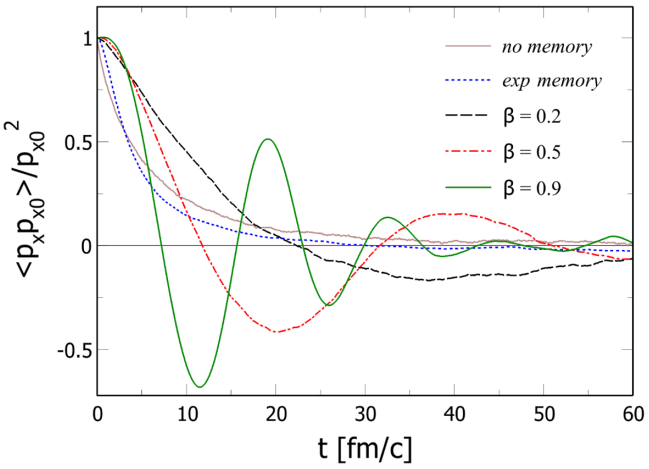

FIG. 3. $\langle p_x \rangle$ versus time for three values of β, $\tau = 1$ fm/c, $p_0 = 1$ GeV, at $T = 1$ GeV and $\mathcal{D} = 0.5$ GeV^2/fm. For the exponential memory (exp memory) calculation, we used $\tau = 1$ fm/c.

cannot be used to estimate quantitatively $\langle p^2(t) \rangle$ in the whole range of β, it is still useful to extract the time dependence of $\langle p^2(t) \rangle$.

We note from Eq. (32) that parametrically $\langle p^2(t) \rangle \propto (t/\tau)^{2\beta} t$. For $t \ll \tau$ the momentum diffusion with $\beta \to 1$ is quite slower than the one with $\beta \to 0$: higher correlations in the noise slow down momentum broadening in the early stage in agreement with [53]. At later times, $t \gg \tau$, Eq. (32) suggests that increasing β results in a faster momentum broadening. This is confirmed by the results shown in Fig. 1 in which the data with large β overshoot those with small β for $t \gg \tau$. We also note that the asymptotic result (32) implies that for $\beta \to 0$ the momentum broadening is independent of τ. Hence, it seems appropriate to state that, in the $\beta \to 0$ limit, we recover the momentum diffusion of a memoryless process.

III. RESULTS

In this section, we present our results on momentum randomization, isotropization, and thermalization of HQs. For illustrative purposes, we first consider a simplified initialization. Then, we show the impact of memory for the more realistic diffusion coefficients, borrowed from pQCD [72,73] and by a quasiparticle model (QPM) [74,75] for several values of T. In the QPM the bulk corresponds to a bath of quasiparticles, that is, quarks and gluons, with temperature-dependent masses. All the results have been obtained by solving Eq. (19), hence taking both diffusion and drag into account.

A. Momentum randomization

In the upper panel of Fig. 3 we plot $\langle p_x p_{x0} \rangle$ in units of p_{x0}^2, where p_{x0} denotes the initial value of p_x, versus time for three values of β, for $\tau = 1$ fm/c, at $T = 1$ GeV and $\mathcal{D} = 0.5$ GeV^2/fm; the results for $\langle p_y p_{y0} \rangle$ and $\langle p_z p_{z0} \rangle$ are similar. The value of $\mathcal{D}$ is about the magnitude of the average diffusion coefficient derived from pQCD at the same temperature and rescaled by the k factor that generates $R_{\rm AA}(p_T)$ which agrees with experimental data in realistic simulations [75]. In the nonrelativistic limit, $\langle p_x p_{x0} \rangle$ is proportional to the autocorrelation function of velocity, which is largely studied in models of stochastic processes with memory kernels. $\langle p_x p_{x0} \rangle$ allows us to study how correlations of momentum with the initial condition are washed out by the interactions of the particle with the bath. For comparison, in this figure we also show one result obtained assuming an exponential memory kernel that follows the implementation of [53], with a memory time $\tau = 1$ fm/c and the same value of $\mathcal{D}$. In Fig. 3 we also show the result for a the calculation for a bath without memory, characterized also by an exponential decay. We note that for the noise with the exponential kernel the behavior of the correlator follows that of the memoryless process, besides a small delay in the very early stage. On the other hand, the behavior of the correlator for the bath with the noise in Eq. (1) is somehow different. For the small $\beta = 0.2$, we find no big qualitative difference between the memoryless and the exponential cases, besides some delay of the momentum randomization: this is not very surprising since we already discussed in the previous section that, for $\beta \to 0$, the correlations of the noise decay quickly. For larger β, $\langle p_x p_{x0} \rangle$ develops oscillations, signaling that the randomization of momentum is nontrivial. It is likely that these oscillations are related to a continuous energy exchange between the bath and the HQ, as it becomes evident from the results on the kinetic energy that we show later. The qualitative behavior of $\langle p_x p_{x0} \rangle$ that we found is in agreement with previous model calculations of the

velocity autocorrelation function in the nonrelativistic limit [76]: in the latter reference, a different memory kernel was used; nevertheless, the trend of the correlator is similar in the two calculations, including the fact that enhancing the correlations of the noise results in wider fluctuations of $\langle p_x p_{x0}\rangle$.

B. Thermalization for a simple initialization

Momentum randomization is not enough to make statements about thermalization: in fact, one should also check that the kinetic energy per particle of the HQs corresponds to the average value expected from a thermal distribution at that temperature $K_{\rm eq}$ given by

$$K_{\rm eq} \equiv \frac{\int \frac{d^3p}{(2\pi)^3}(\sqrt{p^2+m^2}-m)e^{-\sqrt{p^2+m^2}/T}}{\int \frac{d^3p}{(2\pi)^3}e^{-\sqrt{p^2+m^2}/T}}. \quad (33)$$

$K_{\rm eq}$ can be computed analytically for any value of T and m by using standard integral representations of the modified Bessel functions, that lead at

$$K_{\rm eq} = 3T\left[1-\frac{m}{3T}+\frac{m}{3T}\frac{K_1(m/T)}{K_2(m/T)}\right]. \quad (34)$$

In the nonrelativistic limit $K_{\rm eq}=3T/2$, while in the ultrarelativistic case $K_{\rm eq}=3T$.

In this subsection, in order to emphasize the qualitative effects of memory on thermalization, we analyze a simple initialization corresponding to $p_T=1$ GeV and $p_z=0$: the latter corresponds to the midrapidity region of realistic collisions. In Fig. 4 we plot $K\equiv\langle\sqrt{p^2+m^2}-m\rangle$ in units of $K_{\rm eq}$ versus time obtained by our calculations for three values of β, $\tau=1$ fm/c, at $T=0.25$ GeV and $\mathcal{D}=0.1$ GeV^2/fm, in agreement with the coefficient computed within the QPM at $p=1$ GeV at the same temperature. Moreover, $K_{\rm eq}\approx 0.44$ GeV corresponds to the equilibrium value for $T=0.25$ and $m=1.5$ GeV. For comparison, we also plot $K/K_{\rm eq}$ for a memoryless process and for a process with an exponentially decaying memory, as we did in Fig. 3.

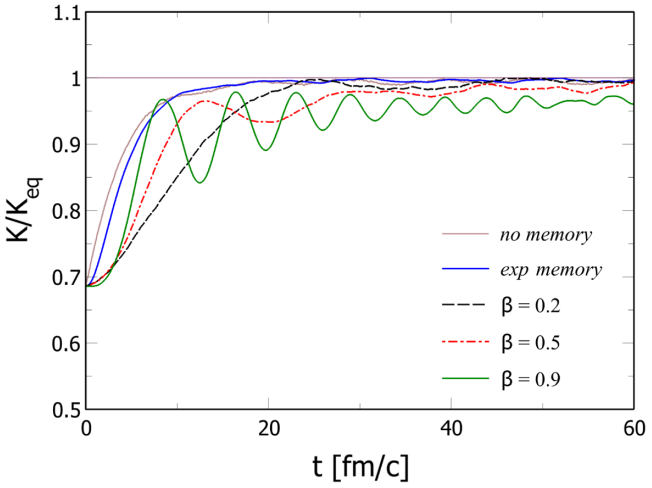

FIG. 4. $K/K_{\rm eq}$ versus time for $\tau=1$ fm/c, at $T=0.25$ GeV and $\mathcal{D}=0.1$ GeV^2/fm. Initialization corresponds to $p_T=1$ GeV and $p_z=0$. The value of $\mathcal{D}$ was chosen in agreement with the diffusion coefficient computed within the QPM at the same temperature and $p=1$ GeV. $K_{\rm eq}=0.44$ GeV.

We note that, for the two smaller values of β in Fig. 4, the average kinetic energy approaches $K_{\rm eq}$ within the time range explored, meaning that the HQs eventually thermalize with the medium; we also note that increasing β from 0.2 to 0.5 results in a few oscillations of $K/K_{\rm eq}$. On the other hand, we note that for $\beta=0.9$ the average kinetic energy of the HQs remains smaller than $K_{\rm eq}$, meaning that in this case thermalization is not complete, due to the correlations of the noise. In contrast, the memoryless and the exponential bath lead eventually to thermalization. We leave the estimate of the thermalization time to the case of realistic initialization in the next subsection: here it is enough to remark that our results suggest that memory in the bath results in the slowing down of thermalization of HQs.

C. Thermalization time for realistic initializations

In the previous subsection, we illustrated the effects of memory on thermalization for charm quarks, using a simplified initialization. In this subsection, we quantitatively study the thermalization time $\tau_{\rm therm}$ of charm and beauty, first focusing on its dependence on $\mathcal{D}$. Different from the previous subsections, here we initialize HQs by means of the realistic fixed order + next-to-leading log (FONLL) distribution [77,78],

$$\left(\frac{dN}{d^2p_T}\right)_{\rm FONLL} = \frac{x_0}{(1+x_3p_T^{x_1})^{x_2}}, \quad (35)$$

where the parameters are $x_0=20.2837$, $x_1=1.95061$, $x_2=3.13695$, $x_3=0.075166$ for charm and $x_0=0.46799$, $x_1=1.83805$, $x_2=3.07569$, $x_3=0.030156$ for beauty. When the bath has no memory, the thermalization time is estimated by studying the decay of one component of the momentum of HQs: in this case, $p_x=p_0e^{-\gamma t}$ with $\tau_{\rm therm}=1/\gamma$. See Fig. 3. When the bath has memory, this definition of $\tau_{\rm therm}$ does not seem to be appropriate, because the average of the components of p fluctuate, see again Fig. 3. Furthermore, more generally, we have already seen that thermalization is delayed with respect to the memoryless case for which $\tau_{\rm therm}=1/\gamma$.

In order to estimate $\tau_{\rm therm}$ in this case, we proceed as follows. We first compute $\langle p_T\rangle$ of HQs corresponding to the initialization in Eq. (35) and assume $p_z=0$ to mimic the midrapidity region of the collisions. Then, we prepare

an initialization with $p_{x0} = \langle p_T \rangle$, $p_{y0} = 0$. For a given $\mathcal{D}$ and T, we compute $\tau_{\rm therm}$ for the bath without memory by fitting $\langle p_x \rangle$ with an exponential function $p_x = p_{x0} e^{-t/\tau_{\rm therm}}$, then we compute $\Upsilon_{\rm therm} \equiv K/K_{\rm eq}$ at $t = \tau_{\rm therm}$; we repeat the procedure for other values of $\mathcal{D}$ at the same T. We find that the value of $\Upsilon_{\rm therm}$ is not very sensitive to the value of $\mathcal{D}$, and that $\tau_{\rm therm} \approx 1/\gamma = \langle E \rangle T/\mathcal{D}$, where $\langle E \rangle$ denotes the initial average energy of HQs from the distribution (35). We then use $\Upsilon_{\rm therm}$ at that T to estimate $\tau_{\rm eq}$ for the bath with memory for each value of $\mathcal{D}$, by identifying in the latter case the thermalization time with the time at which $K/K_{\rm eq} = \Upsilon_{\rm therm}$.

In Fig. 5 we plot $\tau_{\rm therm}$ versus $\mathcal{D}$ for charm quarks at $T = 0.3$ GeV; we checked that the behavior is qualitatively similar for other temperatures as well as for beauty quarks. For the bath with memory, we show the data for the case $\beta = 0.5$ only, since the other cases are qualitatively similar. As already mentioned, for the bath without memory, we find $\tau_{\rm therm} \approx \langle E \rangle T/\mathcal{D}$, in agreement with the fluctuation-dissipation theorem (FDT). For $\beta = 0.5$ we find $\tau_{\rm therm} \propto 1/\mathcal{D}^{\alpha}$ with $\alpha \approx 0.5$. In order to quantify the effect of memory on $\tau_{\rm therm}$, we consider the phenomenologically relevant $\mathcal{D}$ within the QPM model at $p = 0$, namely, this gives $\mathcal{D} = 0.13$ GeV^2/fm at $T = 0.3$ GeV (k factors included). With this value of $\mathcal{D}$, for the bath without memory, we get $\tau_{\rm therm} = 6.9$ fm/c at $T = 0.3$ GeV, while for the bath with memory, we get $\tau_{\rm therm} = 11.4$ fm/c at the same temperature.

In Fig. 6 we plot $\tau_{\rm therm}$ versus T for charm (upper panel) and beauty (lower panel). At each temperature, the diffusion coefficient is that of the QPM model computed at $p = 0$. For the sake of comparison, we also plot the blue circles corresponding to

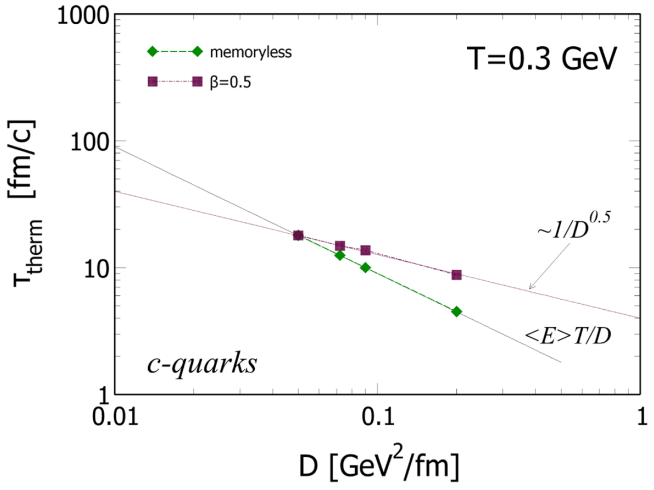

FIG. 5. $\tau_{\rm therm}$ versus $\mathcal{D}$ for charm quarks at $T = 0.3$ GeV. Green diamonds correspond to the bath without memory, while maroon squares correspond to that with a power law memory with $\beta = 0.5$.

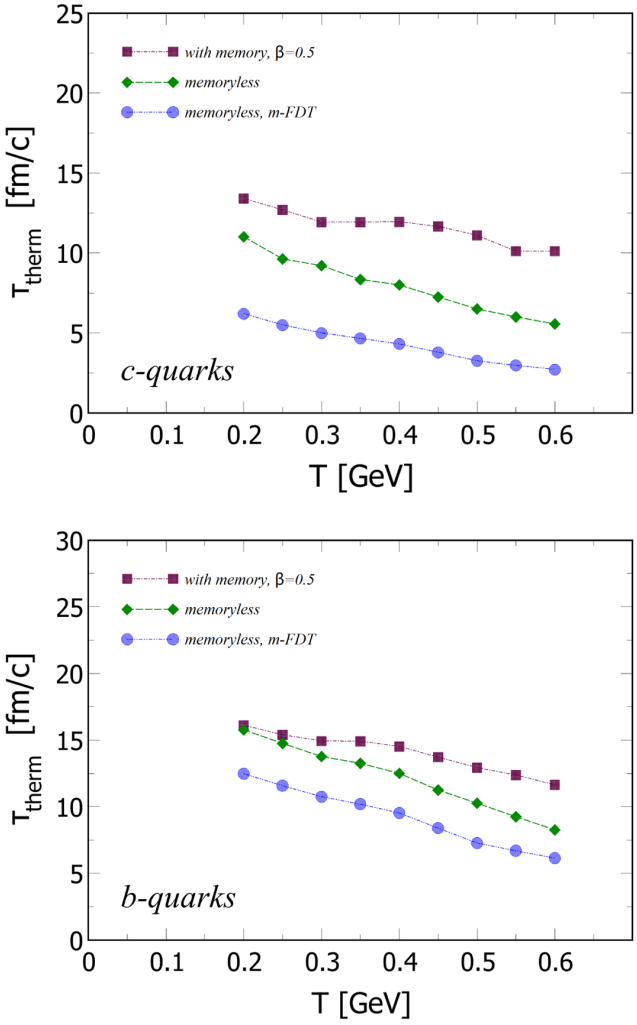

FIG. 6. $\tau_{\rm therm}$ versus T for charm (upper) and beauty (lower). Maroon squares correspond to the thermalization time obtained with memory for $\beta = 0.5$. Green diamonds denote the memoryless thermalization time computed by fitting $p_x(t)$ by $p_x = p_0 e^{-t/\tau_{\rm therm}}$. Finally, blue circles correspond to $\tau_{\rm therm} = 1/\gamma$, with γ computed by Eq. (23) in which we replaced E by m.

$$\tau_{\rm therm} = \frac{mT}{\mathcal{D}}, \tag{36}$$

that amounts to replacing E by m in the FDT (23). We note that already taking into account the initial average kinetic energy of the HQs amounts to an increase of $\tau_{\rm therm}$ in comparison with the result that we would get if we defined $\tau_{\rm therm}$ by virtue of Eq. (36). Finally, the maroon squares correspond to $\tau_{\rm therm}$ for the medium with memory; for the sake of concreteness, we only show the results for $\beta = 0.5$. In this case, $\tau_{\rm therm}$ was defined by comparing $K/K_{\rm eq}$ in the cases with and without memory as explained above. We note that the effect of memory is to increase the thermalization time of HQs; the difference between the cases with and without memory increase with temperature and is milder for beauty quarks.

We can define an effective spatial diffusion coefficient D_s^* by virtue of the relation

$$D_s^* = \frac{T}{\langle E \rangle} \tau_{\rm therm}, \tag{37}$$

where $\langle E \rangle$ denotes the initial average energy of the HQs; the definition (37) gives back the commonly used $D_s = T^3/\mathcal{D}$ when $\tau_{\rm therm} = mT/\mathcal{D}$ and $\langle E \rangle$ is replaced by m. In Fig. 7 we plot $2\pi T D_s^*$ versus T for charm and beauty quarks. Results are shown for the memoryless case as well as for the memory case. We note that the memory in the bulk leads at the increase of D_s^*; the effect is more important for the charm quarks, and the discrepancy between the results obtained with and without memory increases with temperature.

Summarizing, the meaning of the results collected in Fig. 7 is that, due to memory effects, the system appears to have a larger D_s^*. It can delay the formation of the $R_{\rm AA}(p_T)$ with memory. To reproduce the same $R_{\rm AA}(p_T)$ with memory as of the case without memory, one needs to reduce the magnitude of D_s^*. Consequently, if one tries to get the spatial diffusion coefficients that fit the experimental data discarding the memory, then one gets larger values of D_s with respect to the real ones. However, it is interesting that for beauty quarks this effect appears to be negligible between T_c and $3T_c$ even considering strong memory $\beta = 0.5$. This is another feature that makes the extraction of $D_s(T)$ for beauty quarks more solid (and directly comparable to lattice QCD).

D. Momentum isotropization

We close this study by briefly analyzing the isotropization of the heavy quarks. In the midrapidity region of realistic collisions, HQs are produced with a finite average p_T and $p_z \approx 0$: the initial condition is therefore anisotropic in momentum, but the interaction of the HQs with the bath might lead to momentum isotropization. We quantify the momentum anisotropy by introducing an eccentricity ε_p as

$$\varepsilon_p = \frac{\langle p_T^2 - 2p_z^2 \rangle}{\langle p_T^2 + p_z^2 \rangle}. \tag{38}$$

In Fig. 8, we plot ε_p versus time for the memoryless process and for the power law memory process with $\beta = 0.5$. Initialization corresponds to the FONLL distribution with $p_z = 0$. Time is measured in units of the thermalization time for the two cases, which corresponds to $\tau_{\rm therm} = 8.3$ fm/c for the memoryless case and $\tau_{\rm therm} = 11.76$ fm/c for the power law memory case. Moreover, we used $T = 0.3$ GeV and $\mathcal{D} = 0.09$ GeV^2/fm corresponding to the diffusion coefficient computed within the QPM at the same temperature and $p = 0$ GeV, in agreement with the value used in the previous subsection to compute the thermalization time. We checked that, for other values of β, ε_p qualitatively behaves similarly.

Initially $\varepsilon_p = 1$, since $p_z = 0$; however, interactions with the medium lead to $\varepsilon_p \to 0$, namely, to momentum isotropization. Assuming that a fair amount of isotropization takes place when $\varepsilon_p = 0.2$, we find that isotropization time $\tau_{\rm iso}$ is $\tau_{\rm iso} \approx 2.54\tau_{\rm therm}$ for the memoryless case, while $\tau_{\rm iso} \approx 2.76\tau_{\rm therm}$ for the $\beta = 0.5$ case. We conclude that, although memory delays both thermalization and isotropization, $\tau_{\rm therm}$ and $\tau_{\rm iso}$ lie in the same ballpark.

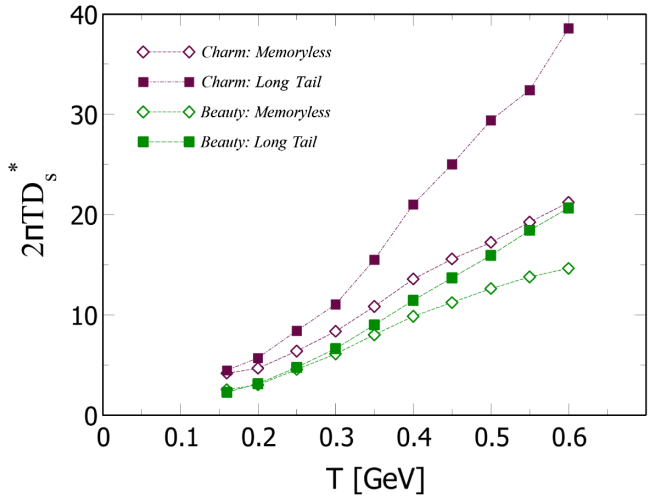

FIG. 7. $2\pi T D_s^*$ versus T for charm and beauty quarks. Open symbols correspond to calculations for the memoryless bulk, solid symbols represent calculations for the bulk with long-tailed memory with $\beta = 0.5$.

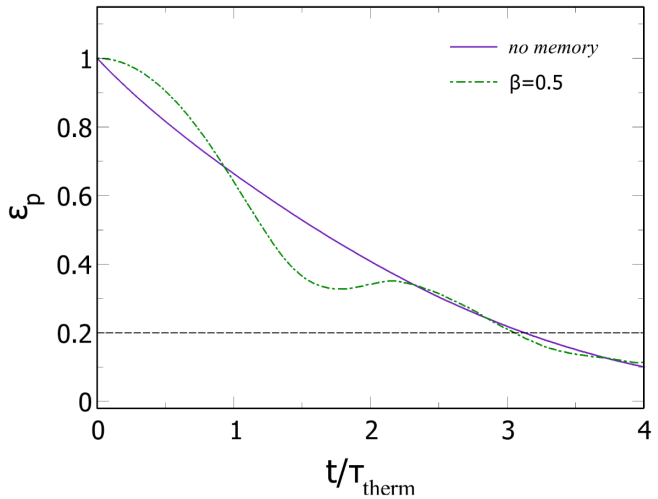

FIG. 8. ε_p versus $t/\tau_{\rm therm}$, at $T = 0.3$ GeV and $\mathcal{D} = 0.09$ GeV^2/fm. Initialization corresponds to the FONLL distribution and $p_z = 0$. The value of $\mathcal{D}$ was chosen in agreement with the diffusion coefficient computed within the QPM at the same temperature and $p = 0$ GeV.

IV. CONCLUSIONS AND OUTLOOK

We studied the effects of a power law correlated noise on momentum randomization, isotropization and thermalization of HQs in a thermal bath. Our work is related to the problem of HQs in relativistic nuclear collisions, in which HQs themselves diffuse and lose energy in the QGP, as well as in the very early stage in which the dynamics of the bulk is dominated by a dense gluon system. This work is a follow-up of [53] in which the same problem was studied, only with the exponential correlator of the random force: in the present work, we focused on a power law correlator. The noise with the desired correlations h was generated by a convenient superposition of Gaussian white noises, see Eq. (1). In this definition, two parameters enter: τ, the memory time, which sets the timescale at which correlations decay [see, for example, Eq. (7)], and β, which changes the power law of the decay of the correlator, see again Eq. (7). Increasing β from 0 to 1 results in the slower decay of the correlator at large times; hence, in some sense, increasing β while keeping τ fixed amounts to having a bath with more persistent memory. The interaction of the heavy quarks with the bath at a fixed temperature was modeled by a generalized Langevin equation, in which the random force η is assumed to be time correlated and the dissipative kernel is defined by a FDT-like equation.

We studied momentum randomization, thermalization, and momentum isotropization of HQs by using the whole Langevin equation (11). Initializing HQs with the particular initial condition $p_x \neq 0$, $p_y = p_z = 0$, we found that the qualitative behavior of $\langle p_x \rangle$ with the power law memory can be quite different from the memoryless case: in fact, the exponential decay expected in the latter case is replaced by damped oscillations in the former case, and the oscillations become more persistent by increasing β. This is in agreement with our general understanding, since increasing β results in injecting more correlations in the random force, hence an HQ needs more time to forget about its initial condition. Our results show that momentum randomization is not a trivial process when HQs interact with a medium with power law memory.

We found that memory slows down thermalization and momentum isotropization of the HQs. Thermalization times are increased by memory: this leads to the increase of the spatial diffusion coefficient. We found that the effect on charm quarks is substantial, while that on beauty quarks is smaller. This is probably due to the fact that, in general, the thermalization times of beauty quarks are larger than those of charms, hence for the former the correlations of the noise have enough time to decay before thermalization sets in. We also found that momentum isotropization is slightly delayed by memory; however, isotropization times starting with the FONLL distribution are in the same ballpark as the thermalization ones.

In the memoryless case, the thermalization time $\tau_{\rm therm}$ is $\propto 1/\mathcal{D}$; on the other hand, in the case of the non-Markovian dynamics, the dependence of $\tau_{\rm therm}$ on $\mathcal{D}$ is different. In particular, for $\beta = 0.5$ we found $\tau_{\rm therm} \propto 1/\mathcal{D}^{0.5}$. This leads to the increase of $\tau_{\rm therm}$ due to memory, which we quantified to be on the order of 30% for the charm quarks for temperatures between T_c and $3T_c$. Interestingly, the impact of memory on $\tau_{\rm therm}$ of beauty quarks is damped in the same range of temperatures in the QGP phase.

This work paves the way to more realistic implementations, which should include a proper initial geometry as well as an expanding medium. In the future, it will be relevant to investigate if the relation between $R_{\rm AA}$ and v_2 is modified by a non-Markovian dynamics and to quantify the potential effects on observables for both charm and beauty quarks. We believe that memory has a potential effect on observables. Following [53] we expect that memory delays the formation of the $R_{\rm AA}(p_T)$; consequently, given a diffusion coefficient and a time interval, memory will keep the values of $R_{\rm AA}(p_T)$ higher. This implies that one would need a higher momentum diffusion coefficient $\mathcal{D}$ or, equivalently, a smaller D_s in order to reproduce the experimental $R_{\rm AA}(p_T)$. In other words, neglecting memory and fixing the transport coefficients in order to reproduce data would lead to an overestimate of D_s. We aim at discussing in detail these problems in future publications.

ACKNOWLEDGMENTS

M. R. acknowledges John Petrucci for inspiration, and V. Minissale, G. Nugara, G. Parisi, S. Plumari, M. L. Sambataro, and, in particular, L. Oliva for the numerous discussions on the topics presented in this article. S. K. D. acknowledges the support from DAE-BRNS, India, Project No. 57/14/02/2021-BRNS. V. G. acknowledges the support from HQCDyn Linea 2 UniCT.

[1] E. V. Shuryak, Nucl. Phys. **A750**, 64 (2005).
[2] B. V. Jacak and B. Muller, Science **337**, 310 (2012).
[3] S. K. Das, P. Palni, J. Sannigrahi, J. e. Alam, C. W. Aung, Y. Bailung, D. Banerjee, G. G. Barnaföldi, S. C. Behera, P. P. Bhaduri *et al.*, Int. J. Mod. Phys. E **31**, 2250097 (2022).
[4] A. Kovner, L. D. McLerran, and H. Weigert, Phys. Rev. D **52**, 6231 (1995).

[5] A. Kovner, L. D. McLerran, and H. Weigert, Phys. Rev. D **52**, 3809 (1995).
[6] T. Lappi and L. McLerran, Nucl. Phys. **A772**, 200 (2006).
[7] J. Cleymans and K. Redlich, Phys. Rev. Lett. **81**, 5284 (1998).
[8] E. V. Shuryak, Nucl. Phys. **A661**, 119 (1999).
[9] M. Golam Mustafa, D. Pal, and D. Kumar Srivastava, Phys. Rev. C **57**, 889 (1998); **57**, 3499(E) (1998).
[10] A. Andronic *et al.*, Eur. Phys. J. C **76**, 107 (2016).
[11] F. Prino and R. Rapp, J. Phys. G **43**, 093002 (2016).
[12] G. Aarts *et al.*, Eur. Phys. J. A **53**, 93 (2017).
[13] R. Rapp, P. B. Gossiaux, A. Andronic, R. Averbeck, S. Masciocchi, A. Beraudo, E. Bratkovskaya, P. Braun-Munzinger, S. Cao, A. Dainese *et al.*, Nucl. Phys. **A979**, 21 (2018).
[14] S. Cao, G. Coci, S. K. Das, W. Ke, S. Y. F. Liu, S. Plumari, T. Song, Y. Xu, J. Aichelin, S. Bass *et al.*, Phys. Rev. C **99**, 054907 (2019).
[15] X. Dong and V. Greco, Prog. Part. Nucl. Phys. **104**, 97 (2019).
[16] Y. Xu, S. A. Bass, P. Moreau, T. Song, M. Nahrgang, E. Bratkovskaya, P. Gossiaux, J. Aichelin, S. Cao, V. Greco *et al.*, Phys. Rev. C **99**, 014902 (2019).
[17] P. B. Gossiaux and J. Aichelin, Phys. Rev. C **78**, 014904 (2008).
[18] J. Uphoff, O. Fochler, Z. Xu, and C. Greiner, Phys. Rev. C **84**, 024908 (2011).
[19] T. Song, H. Berrehrah, D. Cabrera, J. M. Torres-Rincon, L. Tolos, W. Cassing, and E. Bratkovskaya, Phys. Rev. C **92**, 014910 (2015).
[20] S. Cao, T. Luo, G. Y. Qin, and X. N. Wang, Phys. Rev. C **94**, 014909 (2016).
[21] S. K. Das, J. M. Torres-Rincon, L. Tolos, V. Minissale, F. Scardina, and V. Greco, Phys. Rev. D **94**, 114039 (2016).
[22] S. Plumari, V. Minissale, S. K. Das, G. Coci, and V. Greco, Eur. Phys. J. C **78**, 348 (2018).
[23] S. K. Das, F. Scardina, S. Plumari, and V. Greco, Phys. Rev. C **90**, 044901 (2014).
[24] H. van Hees, V. Greco, and R. Rapp, Phys. Rev. C **73**, 034913 (2006).
[25] H. Van Hees, M. Mannarelli, V. Greco, and R. Rapp, Phys. Rev. Lett. **100**, 192301 (2008).
[26] S. K. Das, J. e. Alam, and P. Mohanty, Phys. Rev. C **82**, 014908 (2010).
[27] W. M. Alberico, A. Beraudo, A. De Pace, A. Molinari, M. Monteno, M. Nardi, and F. Prino, Eur. Phys. J. C **71**, 1666 (2011).
[28] M. He, R. J. Fries, and R. Rapp, Phys. Rev. Lett. **110**, 112301 (2013).
[29] M. He, H. van Hees, P. B. Gossiaux, R. J. Fries, and R. Rapp, Phys. Rev. E **88**, 032138 (2013).
[30] S. Cao, G. Y. Qin, and S. A. Bass, Phys. Rev. C **92**, 024907 (2015).
[31] T. Lang, H. van Hees, J. Steinheimer, G. Inghirami, and M. Bleicher, Phys. Rev. C **93**, 014901 (2016).
[32] S. K. Das, S. Plumari, S. Chatterjee, J. Alam, F. Scardina, and V. Greco, Phys. Lett. B **768**, 260 (2017).
[33] Y. Xu, J. E. Bernhard, S. A. Bass, M. Nahrgang, and S. Cao, Phys. Rev. C **97**, 014907 (2018).
[34] R. Katz, C. A. G. Prado, J. Noronha-Hostler, J. Noronha, and A. A. P. Suaide, Phys. Rev. C **102**, 024906 (2020).
[35] S. Li, W. Xiong, and R. Wan, Eur. Phys. J. C **80**, 1113 (2020).
[36] M. Nahrgang, J. Aichelin, S. Bass, P. B. Gossiaux, and K. Werner, Phys. Rev. C **91**, 014904 (2015).
[37] T. Song, H. Berrehrah, D. Cabrera, W. Cassing, and E. Bratkovskaya, Phys. Rev. C **93**, 034906 (2016).
[38] S. K. Das, M. Ruggieri, F. Scardina, S. Plumari, and V. Greco, J. Phys. G **44**, 095102 (2017).
[39] J. H. Liu, S. Plumari, S. K. Das, V. Greco, and M. Ruggieri, Phys. Rev. C **102**, 044902 (2020).
[40] J. H. Liu, S. K. Das, V. Greco, and M. Ruggieri, Phys. Rev. D **103**, 034029 (2021).
[41] P. Khowal, S. K. Das, L. Oliva, and M. Ruggieri, Eur. Phys. J. Plus **137**, 307 (2022).
[42] B. Schenke and C. Greiner, Phys. Rev. Lett. **98**, 022301 (2007).
[43] J. I. Kapusta, B. Muller, and M. Stephanov, Phys. Rev. C **85**, 054906 (2012).
[44] J. I. Kapusta and J. M. Torres-Rincon, Phys. Rev. C **86**, 054911 (2012).
[45] J. Schmidt, A. Meistrenko, H. van Hees, Z. Xu, and C. Greiner, Phys. Rev. E **91**, 032125 (2015).
[46] K. Murase and T. Hirano, Nucl. Phys. **A956**, 276 (2016).
[47] J. I. Kapusta and C. Plumberg, Phys. Rev. C **97**, 014906 (2018); **102**, 019901(E) (2020).
[48] J. Hammelmann, J. M. Torres-Rincon, J. B. Rose, M. Greif, and H. Elfner, Phys. Rev. D **99**, 076015 (2019).
[49] F. A. Oliveira, R. M. S. Ferreira, L. C. Lapas, and M. H. Vainstein, Front. Phys. **7**, 18 (2019).
[50] M. Ruggieri, M. Frasca, and S. K. Das, Chin. Phys. C **43**, 094105 (2019).
[51] B. Schüller, A. Meistrenko, H. Van Hees, Z. Xu, and C. Greiner, Ann. Phys. (Amsterdam) **412**, 168045 (2020).
[52] W. Chen, C. Greiner, and Z. Xu, Phys. Rev. E **107**, 064131 (2023).
[53] M. Ruggieri, Pooja, J. Prakash, and S. K. Das, Phys. Rev. D **106**, 034032 (2022).
[54] R. Metzler and J. Klafter, Phys. Rep. **339**, 1 (2000).
[55] I. M. Sokolov and J. Klafter, Chaos **15**, 026103 (2005).
[56] L. Vlahos, H. Isliker, Y. Kominis, and K. Hizanidis, arXiv:0805.0419v1.
[57] W. Chen, H. Sun, X. Zhang, and D. Korošak, Comput. Math. Appl. **59**, 1754 (2010).
[58] S. Bhattacharya, S. K. Banik, S. Chattopadhyay, and J. R. Chaudhuri, J. Math. Phys. (N.Y.) **49**, 063302 (2008).
[59] M. Vogt and R. Hernandez, J. Chem. Phys. **123**, 144109 (2005).
[60] R. Hernandez, J. Chem. Phys. **111**, 7701 (1999).
[61] R. Hernandez and F. L. Somer, Jr., J. Phys. Chem. B **103**, 1064 (1999).
[62] R. Hernandez and F. L. Somer, Jr., J. Phys. Chem. B **103**, 1070 (1999).
[63] F. L. Somer, Jr. and R. Hernandez, J. Phys. Chem. B **104**, 3456 (2000).
[64] A. V. Popov and R. Hernandez, J. Chem. Phys. **126**, 244506 (2007).
[65] S. Kawai and T. Komatsuzaki, J. Chem. Phys. **134**, 114523 (2011).

[66] H. Meyer, T. Voigtmann, and T. Schilling, J. Chem. Phys. **147**, 214110 (2017).
[67] I. Prigogine, *Non-Equilibrium Statistical Mechanics* (Dover Publications, New York, 2017).
[68] R. Zwanzig, *Nonequilibrium Statistical Mechanics* (Oxford University Press, New York, 2001).
[69] R. Kubo, Rep. Prog. Phys. **29**, 255 (1966).
[70] D. B. Walton and J. Rafelski, Phys. Rev. Lett. **84**, 31 (2000).
[71] R. Rapp and H. van Hees, arXiv:0903.1096.
[72] B. L. Combridge, Nucl. Phys. **B151**, 429 (1979).
[73] B. Svetitsky, Phys. Rev. D **37**, 2484 (1988).
[74] S. K. Das, F. Scardina, S. Plumari, and V. Greco, Phys. Lett. B **747**, 260 (2015).
[75] F. Scardina, S. K. Das, V. Minissale, S. Plumari, and V. Greco, Phys. Rev. C **96**, 044905 (2017).
[76] G. R. Kneller, J. Chem. Phys. **134**, 224106 (2011).
[77] M. Cacciari, M. Greco, and P. Nason, J. High Energy Phys. 05 (1998) 007; M. Cacciari, S. Frixione, and P. Nason, J. High Energy Phys. 03 (**2001**) 006.
[78] M. Cacciari, S. Frixione, N. Houdeau, M. L. Mangano, P. Nason, and G. Ridolfi, J. High Energy Phys. 10 (2012) 137.